PCCP

Cite this: *Phys. Chem. Chem. Phys.*, 2012, **14**, 4977–4984

www.rsc.org/pccp

PAPER

Electronic excitation spectra of the $[Ir(ppy)_2(bpy)]^+$ photosensitizer bound to small silver clusters Ag_n (n = 1–6)†

Olga S. Bokareva,* Sergey I. Bokarev and Oliver Kühn

Received 3rd January 2012, Accepted 17th February 2012
DOI: 10.1039/c2cp00011c

The changes in nature and order of the excited electronic states of the photosensitizer $[Ir(ppy)_2(bpy)]^+$ upon binding to small silver clusters, Ag_n (n = 1–6), were studied theoretically using the linear response TDDFT method with the range-separated LC-BLYP functional. Binding energies and localization of HOMO and LUMO orbitals are found to oscillate with the number of silver atoms. Special emphasis is put on the discussion of long-range charge transfer transitions between the photosensitizer and the silver cluster. The energies of these transitions were found to be only slightly dependent on the relative orientations of both fragments, but strongly dependent on the intermolecular distance. The absorption spectrum of the combined system does not show a systematic trend with respect to cluster size, but it is strongly modified by the charge transfer transitions. Possible photophysical processes of the systems containing larger clusters are discussed.

Introduction

Combination of metal nanoparticles with molecular adsorbates like organic dyes, semiconductors, and J-aggregates is a well-known and prospective way to design and tune functional properties of new nano-scaled materials (*e.g.* ref. 1–3). Such designed materials could be exploited in biosensors,[4] biomolecular electronics, photocatalysis,[5] drug delivery *etc.* Various interaction mechanisms can be responsible for the unique behaviour of such combined systems. Depending on composition and arrangement, metal nanoparticles can either enhance (through the local field/surface plasmon effect) or quench the fluorescence and absorption of adsorbates[6,7] as well as its Raman scattering.[8–10] Conversely, molecular adsorbates can shift the surface plasmon peak position and consequently modify the optical properties of the nanoparticle. In the case of strong interaction, the mutual influence can lead to the appearance of a completely new material with characteristics not observed for the constituents.[11]

Besides the study of large nanoparticles, smaller ones with molecular-like excitations also gained attention because of their effective light emission under UV-vis excitation (see *e.g.* ref. 12 and 13). Upon reduction of the cluster size the nature of transitions changes from plasmonic to molecular-like.[14] Theoretical investigations of systems including small nanoparticles cover a wide range of adsorbates such as small organic molecules[15] and peptides.[3]

Institute of Physics, University of Rostock, Universitätsplatz 3, D-18055 Rostock, Germany. E-mail: olga.bokareva@uni-rostock.de; Fax: +49-381-498-6942
† Electronic supplementary information (ESI) available. See DOI: 10.1039/c2cp00011c

In this paper, we present a computational study of the electronic spectra of $[Ir(ppy)_2(bpy)]^+$ denoted IrPS (Fig. 1) bound to small silver clusters, Ag_n (n = 1–6). The tuning of photophysical and photochemical properties of photosensitizers containing noble metals is of special interest from the viewpoint of light emitting devices[16] and photocatalysis, in particular photo-production of hydrogen.[17–22] In the present case, the focus on the particular Ir(III) complex is related to the activities of Beller and co-workers[21] who developed an effective photocatalytic system for water splitting by combining IrPS with the sacrificial reductant triethylamine and a water reduction iron catalyst. In the first stage of the catalytic cycle, IrPS is photoexcited. Subsequently, effective intersystem crossing[23,24] may lead to relaxation to the lowest triplet state, which then reacts with the electron donor triethylamine. Further, the reduced $[Ir(ppy)_2(bpy)]^0$ form reacts with the iron catalyst responsible for water reduction.

The spectroscopy of such organometallic compounds is usually discussed on the basis of ligand-centred (LC) and metal-to-ligand charge-transfer (MLCT) excited electronic states. For IrPS, the ordering of LC and MLCT states is known

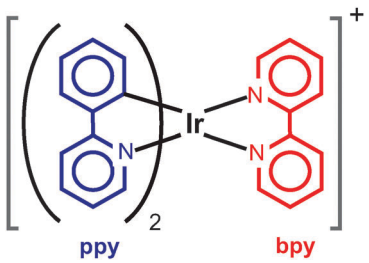

Fig. 1 Chemical structure of $[Ir(ppy)_2(bpy)]^+$ (IrPS).

to depend strongly on the environment (solvent and temperature).[25] Under certain conditions, *i.e.* when excited states are close in energy, the luminescence from several states can be detected simultaneously.[25–27]

In our previous study on the bare IrPS,[28] we assigned the absorption spectrum on the basis of LC-BLYP calculations. The weak bands in the region between 2.5 and 3.7 eV were attributed to singlet–triplet MLCT and LC transitions. A shoulder at about 3.7–4.3 eV corresponds to two strong singlet–singlet MLCT transitions and bands at about 4.3–5.0 eV consist of several strong LC transitions on the diffuse background of the strong and medium intensity MLCT bands.

In the present paper, we extend our study on the electronic properties of IrPS. In particular we will focus on changes in the nature and order of the excited electronic states upon binding to small silver clusters. One possibility would be that upon photoexcitation there is a charge separation, *i.e.* an intermolecular (IM) transition between IrPS and Ag_n. This, of course, could have a considerable impact on the efficiency of the photosensitizer and it could point towards the design of alternative catalytic cycles.

In the following section, we will give details of the computational approach. Subsequently, results on electronic ground state geometries and binding energies of various cluster–IrPS complexes are presented. This is followed by an account on vertical electronic excitation spectra. In the Discussion section, we put emphasis on possible implications of changes in the low-energy part of the spectrum on the photophysical behaviour for systems with larger silver clusters.

Computational details

All calculations were performed using the LANL2DZ ECP and basis set for Ir and Ag[29] and the 6-31G(d) basis[30,31] for all other atoms. In order to cope with the problem of charge-transfer (CT),[32,33] DFT/TDDFT with the range-separated density functional, LC-BLYP,[34–36] was the main theoretical approach used in this work. In our previous study on bare IrPS,[28] this method was shown to give excitation energies in good agreement with experimental data and results of CASSCF/CASPT2 calculations. At this theoretical level, the geometries of the ground electronic state of IrPS$\cdots$$Ag_n$ and vertical electronic excitation spectra were calculated. For the purpose of comparison, some other functionals were utilised for the calculation of vertical electronic excitation spectra, namely: PBE0,[37–39] BHHLYP,[40] CAM-B3LYP,[41] and M06-HF.[42] Since M06-HF is known to be slowly convergent and give large errors if a small grid is used,[43] the number of grid points was increased for this functional (120 radial points and 2030 points in the Lebedev grid) as compared to other functionals (96 and 302, respectively). The standard μ parameter value of 0.33 $Bohr^{-1}$ for the long-range correction scheme in LC-BLYP and coulomb attenuated B3LYP was used. The counterpoise method[44,45] was used to correct the basis set superposition error (BSSE); each of the units was calculated with the basis functions of the other fragment, using so-called ghost orbitals. For DFT/TDDFT calculations no symmetry restrictions were applied. In the current study, the energies of the triplet states were calculated without accounting for spin–orbit coupling, thus, there are no oscillator strengths for the respective transitions. All calculations have been performed with the GAMESS US[46] program package.

In order to find the preferable sites for the binding of the IrPS to the silver clusters we estimated (LC-BLYP) the total energies of Ag_2 clusters placed on the spheres with radii 4.0, 6.0, and 8.0 Å with the Ir^{3+} ion in the centre in such a way that the bond axis of Ag_2 coincides with the radial direction. Unphysical configurations corresponding to overlap of atoms were excluded. In addition, we obtained 200–400 random trial geometries for larger clusters (n = 4 and 6) with smallest r(Ag–Ir) varying from 2.0 to 8.0 Å and fixed distances r(Ag–Ag) = 2.7 Å; overlapping structures were excluded. The obtained lowest energy geometric configurations were further utilised as starting for the geometry optimisations.

In principle we could identify two binding types, *i.e.* "edge" binding between the metal cluster and terminal hydrogen atoms of the ligands and "cavity" binding where a silver cluster is placed either in the unique "ppy–ppy" cavity between two ppy ligands or in one of two "bpy–ppy" cavities. In both cases, the interaction is "weak" and no chemical bonds are formed.

For comparison, the equilibrium structures of the isolated silver clusters, Ag_n (n = 3–6), have also been optimised using DFT/LC-BLYP, starting from geometries reported in ref. 47–52. The results are compiled in Table S1 of the ESI.† In general, we observe that LC-BLYP predicts shorter bond length (by 0.02–0.03 Å) as compared with other functionals. However, conformational energy differences are in reasonable agreement with coupled cluster calculations.[48]

Results

Ground electronic state

The results of the geometry optimization of IrPS$\cdots$$Ag_n$ structures indicate that configurations in which Ag_n is situated in the cavities between ligands are the lowest in energy, see Fig. 2. Important geometry parameters are summarised in Table 1. We note in passing that in some cases, the C_2 point symmetry of the bare IrPS part[53] was retained upon optimisation of the complex, although it was carried out without symmetry constraints.

The relative positions of IrPS and Ag_n and BSSE corrected binding energies can be seen from Fig. 2. Our focus will be on structures of "ppy–ppy" binding type. The conformers with the same number of silver atoms are labelled in order of decreasing binding energy (*e.g.* IVa, IVb,...). In general, the complexes correspond to cases of weak interaction of Ag_n with IrPS, with binding energies being 10 times smaller compared to those of silver atoms in large nanoparticles.[54] Accounting for the BSSE in most cases decreased the binding energies by about 4 to 11 kJ mol^{-1} with three exceptions (I, III, and Va), where E_b increased by about 24, 3, and 9 kJ mol^{-1} per silver atom, respectively. Overall, we notice that binding energies oscillate with increasing number of silver atoms (see Fig. 2).

The most notable changes in IrPS geometry upon complexation are observed for the systems with odd number of silver atoms for $r(C–C)_{bpy}$, $r(Ir–N_{bpy})$, and $r(Ir–C_{ppy})$, see Table 1 (maximal changes are 0.07 Å and 7.6°). In the case of an even number of silver atoms, only minor changes are observed.

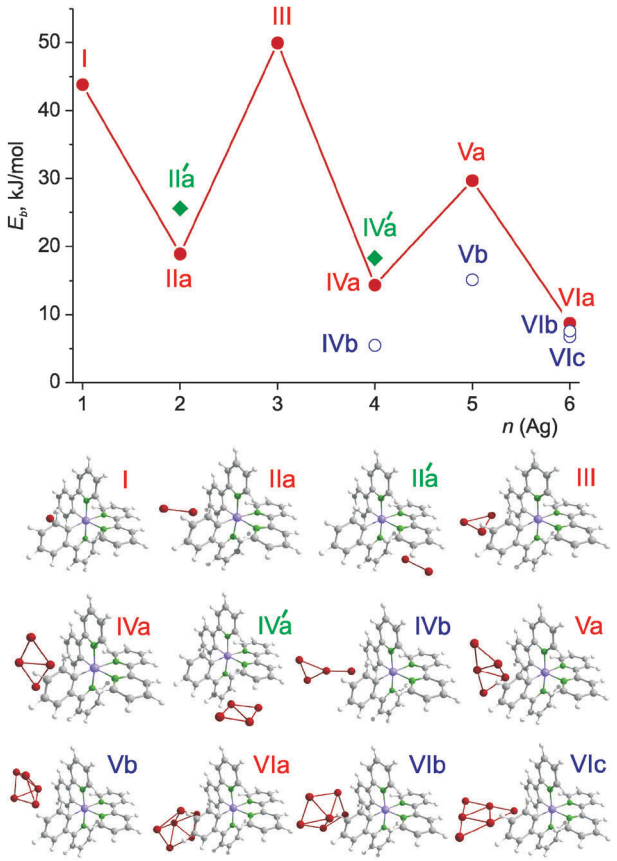

Fig. 2 BSSE corrected binding energies per 1 silver atom, structures, and notations of optimized systems IrPS···Ag_n (n = 1–6). Red line is guide for eyes connecting structures of "ppy–ppy" type under discussion (red circles, labels I, IIa,...); structures of "bpy–ppy" type are marked with green diamonds (labels II′a, IV′a).

In contrast, interaction with IrPS leads to pronounced changes in cluster geometries as compared with the isolated case, both for odd and even numbers of Ag atoms. Most notable are changes in bond lengths for n = 2, 3, and 5 by up to 0.25 Å. In addition, the initially planar Ag_5 cluster becomes significantly non-planar (structure Va).

The weak binding between silver clusters and IrPS can also be classified according to their relative orientation. In most cases clusters tend to orient in the cavities in such a way that one of the vertices lies closer to the Ir^{3+} center than the others. Exceptions are structures III, VIa, and VIb, where clusters are aligned along the ppy ligands.

For the purpose of comparison, we optimized alternative configurations, where Ag_2 and Ag_4 (D_{2h}) clusters were located in the ppy–bpy cavity; see ESI.† Binding energies of IIa and IVa are higher by about 5 kJ mol^{-1} (per silver atom) relative to IIa and IVa (see Table S2, ESI†). Note that structures IIa and IVa are also aligned along ppy and bpy ligands.

The character of frontier orbitals in the energy range from −2 to −9 eV for the structures with the largest binding energies is shown in Fig. 3. Analysing the shape of HOMO and LUMO, the difference between systems with odd and even numbers of silver atoms can be explained by the different structure of the ground electronic state. The character of HOMO and LUMO of the complexes varies: for systems with odd n the HOMO is a half-occupied π*(bpy) orbital and the LUMO is a σ* orbital of the silver cluster (Fig. 3); for even n the situation is reversed—the HOMO is localized at the silver moiety and the LUMO at the bpy ligand. In other words, the clusters with odd n = 1, 3, and 5 reduce the readily reducible bpy ligand resulting in a $[Ir(ppy)_2(bpy^{-\bullet})]^0\cdots Ag_n^+$ configuration of the ground electronic state with a closed-shell Ag_n^+ cluster. This means that for odd n long-range charge transfer from silver cluster to IrPS occurs already in the ground electronic state. An exception is the Vb structure: according to geometry and orbital structure it belongs to the "even" group. Differences in geometric parameters of IrPS (see Table S3, ESI†) are in accord with this observation.

From Fig. 3, one can see an oscillating dependence of HOMO–LUMO gap on the number of silver atoms. The changes of gaps are mostly due to the changes in HOMO positions while the LUMO energy is practically the same for most structures although the nature of the orbital does change. These oscillations come along with similar changes of other properties like geometrical parameters and binding energies (Table 1 and Fig. 2). Such a behaviour (*e.g.* oscillations of average bond length, energy difference between dissociation energies of preferable channels) is a known feature of small metal clusters.[54]

Vertical electronic excitation spectra. Comparison of different methods for the system IIa

The particular assignment and main features of the electronic absorption spectra will be discussed in the next paragraph. Here we focus on the comparison of different DFT functionals

Table 1 Selected equilibrium geometry parameters of IrPS and IrPS···Ag_n (for notation see Fig. 2) in the ground electronic state (LC-BLYP). Bond lengths in Å, angles in degrees

Parameter	IrPS[28]	I	IIa	III	IVa	Va	VIa[b]
Symmetry	C_2	C_2	C_2	~C_2	C_2	C_2	C_1
r(Ir–C_{ppy})	2.007	2.028	2.008	2.009	2.009	2.001	2.004 (2.006)
r(Ir–N_{ppy})	2.055	2.055	2.056	2.048	2.057	2.050	2.057 (2.058)
r(Ir–N_{bpy})	2.163	2.112	2.161	2.122	2.160	2.121	2.156 (2.164)
r(C–C)$_{ppy}$	1.463	1.473	1.465	1.472	1.466	1.474	1.463 (1.467)
r(C–C)$_{bpy}$	1.485	1.415	1.485	1.415	1.485	1.415	1.485
r(Ir–Ag)[a]	—	3.333	3.808	4.856	3.665	4.102	4.626
r(Ag–Ag)	—	—	2.552	2.640–2.721	2.684–2.771	2.652–2.987	2.718–2.888
∠ CIrC	89.3	91.8	90.4	88.7	92.1	90.4	89.1
∠ $N_{ppy}IrN_{ppy}$	172.1	179.7	172.0	175.5	173.4	174.0	170.5
d(CIrCN)	94.2	99.5	94.1	97.0	94.7	95.4	93.1

[a] Closest Ir–Ag distance. [b] Parameters of the ppy fragment closest to the Ag cluster (second ppy fragment in parentheses).

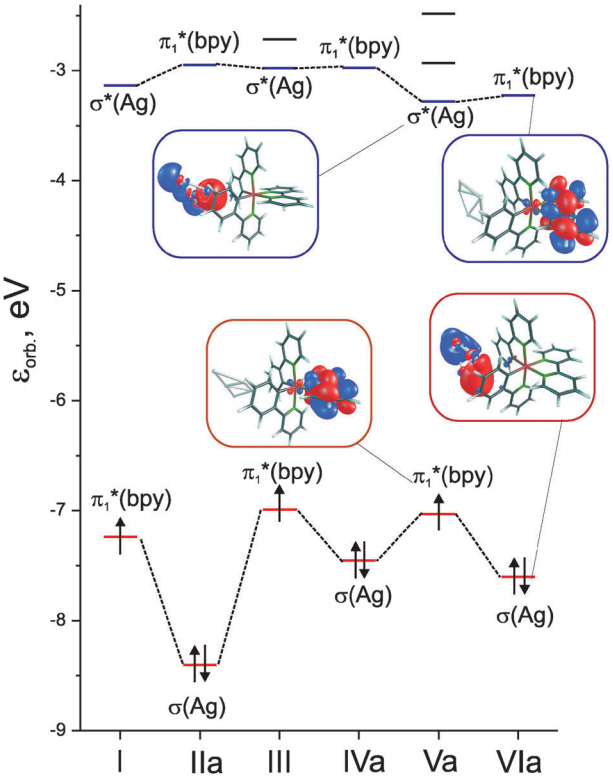

Fig. 3 Frontier orbitals (contour value 0.03) for IrPS···Ag_n systems.

for the case of structure IIa. Based on the results obtained for the bare IrPS[28] and the structures of the frontier orbitals (see Fig. 3) we expect the presence of long-range charge-transfer electronic IM transitions between IrPS and Ag_n. Therefore, we have performed a study of the dependence of selected vertical excitation energies on the extent of the exact exchange in the DFT functional. Specifically, we have used the following functionals (amount of exact exchange in parentheses): BLYP (0%), PBE0 (25%), BHHLYP (50%), CAM-B3LYP (19–65%), LC-BLYP (0–100%), and M06-HF (100%). The results are summarised in Table 2. Note that some transitions have not been found among the lowest excited states considered or cannot be unambiguously assigned.

As for the bare IrPS,[28] there is a systematic trend: the higher the extent of HF exchange, the higher the CT transition energies. In the case of the $\sigma(Ag) \rightarrow \pi_1^*(bpy)$ transition this trend is more pronounced than for other CT excitations because for this transition the charge separation is most long-ranged in complex IIa and the overlap of wave functions of donor and acceptor moieties is almost zero. For the correlation of orbital overlap and error for CT states see ref. 33. In contrast, the purely local excitation $\sigma(Ag) \rightarrow \sigma^*(Ag)$ is similarly predicted by different functionals with M06-HF as an exception, where this transition is the lowest. It is interesting to note that range-separated functionals LC-BLYP and CAM-B3LYP give results close to each other as well as to BHHLYP. This means that a notable amount of HF-exchange energy in DFT could allow us to get satisfactory results when compared to long-range corrected functionals. However, the incorrect R dependence of the CT potential curves[32] (see below) can be attributed to the deficiencies of BHHLYP. We will draw our main conclusions on the basis of the range-separated LC-BLYP functional since it was utilized as the main method for the free IrPS.[28]

Changes in absorption spectra upon binding

The changes in absorption spectra upon complexation of IrPS and Ag_n can be seen in Fig. 4a and corresponding numbers and assignments are given in Tables 3 and 4 for transitions localized on IrPS and Ag_n, respectively. For comparison, we also show spectra of isolated IrPS and Ag_n. Note that in cases I, III and Va we compare the spectra of reduced $IrPS^0$ and oxidized Ag_n^+ according to the results on the structure of the ground electronic state. In general, the influence of the formation of the intermolecular complex upon absorption is not strong when considering the IrPS transitions alone. As a rule the transition energies increase by up to 0.31 eV with respect to isolated IrPS, see Table 3. Exceptions are the doublet–doublet transitions $\pi_1^*(bpy) \rightarrow \pi_1^*(ppy)$ and $\pi_1^*(bpy) \rightarrow \pi_2^*(ppy)$ for system I, which show a decrease by 0.4–0.6 eV. Note that the energy of the doublet–doublet $d_{x^2-y^2} \rightarrow \pi_1^*(ppy)$ for system III is shifted upon interaction by about 0.8 eV to the blue with a dramatic increase of the oscillator strength. However, no systematic increase of the intensities is observed for the IrPS intensities (Table 3).

Changes in bare silver cluster transitions are also not systematic. In Table 4, the most intense transitions for pure and bound silver clusters are collected, being mostly of $\sigma \rightarrow \sigma^*$ character. Binding of Ag_n to IrPS leads to the loss of symmetry of cluster orbitals which makes the correspondence between transitions in pure and bound clusters not always unambiguous. There are cases where the energy of a transition changes by 0.01–0.37 eV to the red or to the blue and the oscillator strength decreases or increases. In some cases, the maximum positions are shifted by 0.62–1.74 eV with a simultaneous decrease of intensity. In general, the influence of the absorbed IrPS on the silver cluster's transitions is more pronounced than changes in IrPS spectra caused by binding to the clusters.

We would like to emphasize that despite the weak interaction between IrPS and Ag_n electronic transitions due to long-range

Table 2 Selected singlet–singlet vertical transition energies (in eV) as well as oscillator strengths calculated with different DFT functionals for system IIa (note that some transitions have not been found among the lowest excited states considered)

	BLYP	PBE0	BHHLYP	CAM-B3LYP	LC-BLYP	M06-HF
$\sigma(Ag) \rightarrow \pi_1^*(bpy)$	0.79 (0.000)	1.32 (0.000)	2.30 (0.000)	2.79 (0.000)	2.92 (0.001)	3.47 (0.027)
$\sigma(Ag) \rightarrow \pi_1^*(ppy)$	1.71 (0.000)	2.10 (0.000)	2.94 (0.000)	3.27 (0.000)	3.00 (0.010)	4.30 (0.055)
$d_{x^2-y^2} \rightarrow \pi_1^*(bpy)$	1.58 (0.000)	2.46 (0.000)	3.47 (0.000)	3.28 (0.000)	3.74 (0.000)	5.12 (0.001)
$d_{x^2-y^2} \rightarrow \pi_1^*(ppy)$	2.56 (0.018)	2.10 (0.000)	3.99 (0.054)	3.81 (0.077)	4.07 (0.120)	—
$d_{yz} \rightarrow \pi_1^*(bpy)$	2.31 (0.000)	3.29 (0.001)	4.42 (0.003)	4.03 (0.001)	4.13 (0.001)	—
$\sigma(Ag) \rightarrow \sigma^*(Ag)$	—	3.06 (0.728)	3.04 (0.756)	3.01 (0.703)	3.36 (0.446)	2.71 (0.645)

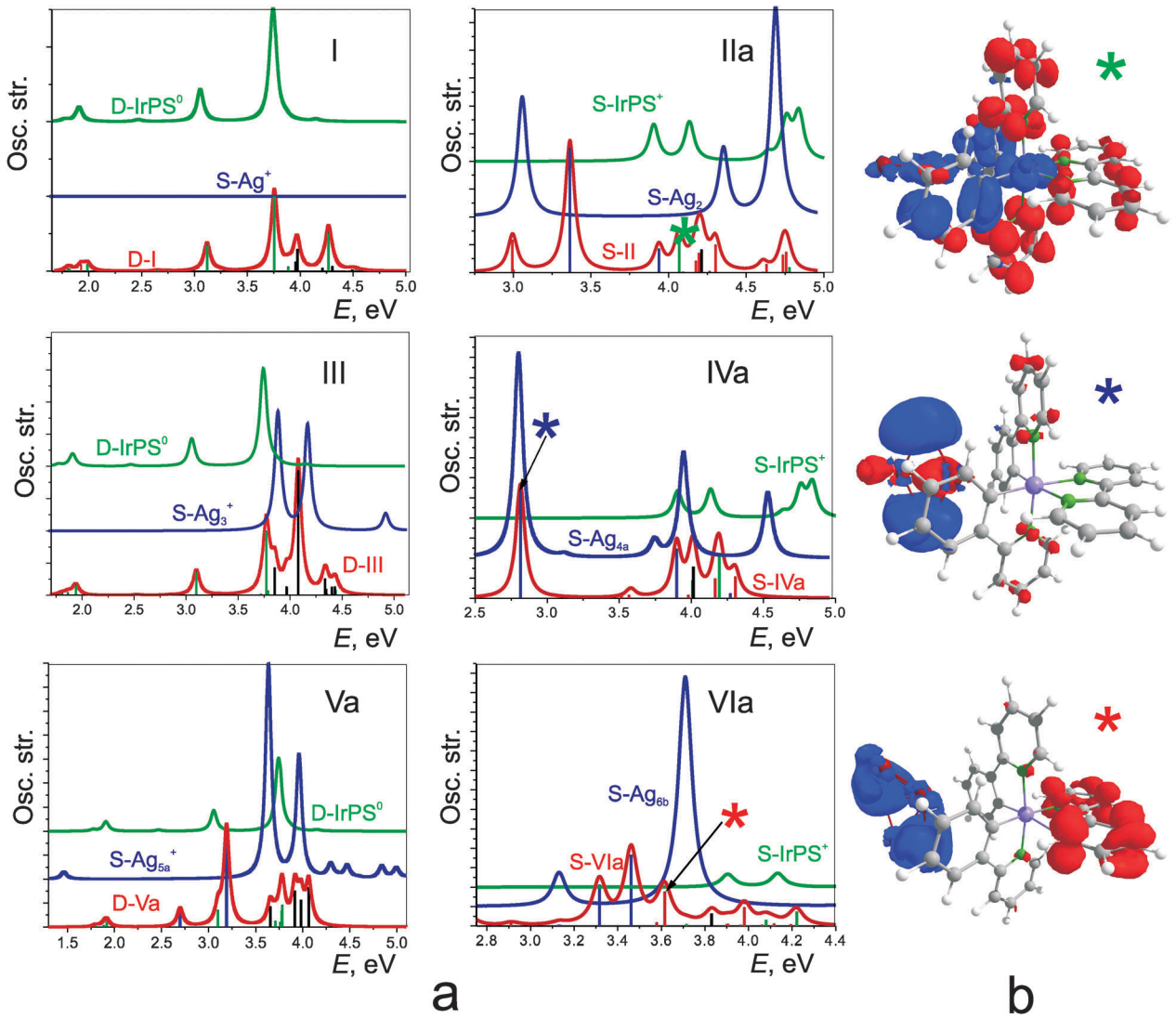

Fig. 4 (a) Comparison of the TDDFT (LC-BLYP) vertical electronic singlet–singlet (S-) and doublet–doublet (D-) spectra of different IrPS$\cdots$Ag$_n$ systems. Vertical bars and associated broadened spectra (Lorentzian of width 0.04 eV) are assigned to transitions of IM (red), IrPS (green), Ag$_n$ (blue). In addition there are transitions of mixed character (black bars). (b) Electron density differences (contour value 0.0008) for selected transitions, which are marked with asterisks in panel (a). Red and blue colors correspond to particle and hole densities, respectively.

CT, IrPS $\rightarrow$ Ag$_n$ or Ag$_n$ $\rightarrow$ IrPS, appeared. In Fig. 4a these transitions are marked with red vertical bars and in Fig. 4b electron density difference plots for the transitions of different types are given. Transitions of IM type are not listed in tables because they can hardly be compared for systems with different n. In general, these transitions are not the most intense ones in the spectrum below 5 eV, but the density of such states is quite high even for small n which leads to the notable changes in the overall shape of the spectrum.

Interestingly, the "bpy–ppy" structures (II′a and IV′a) have a similar structure of the low-energy part of the absorption spectrum, see ESI.† This hints that the mutual orientation may play a minor role and the determining factor is the distance (see next section) between silver cluster and IrPS.

Distance dependences of energy spectra

In Fig. 5, the dependence of the energy of the lowest excited singlet and triplet electronic states on the distance between Ir and the closest Ag atom is presented. The curves are constructed on the basis of seven single point calculations with the geometries taken from the ground electronic state minimization. Only those states, which are common for all points are presented. Note that some Ag $\rightarrow$ IrPS CT transitions are present among the lowest states only for points close to the minimum. Their energy goes up very fast with increasing distance. Due to the use of the range-separated LC-BLYP functional, which shows a correct behaviour at large distances,[32] potential curves of excited CT states are well approximated by a $1/R$ dependence. Due to this behaviour the number of localized states among the 15 lowest ones increases with distance. Note that while BHHLYP is giving results close to LC-BLYP for the IIa minimum, it predicts a much flatter R dependence of the CT potential curves (not shown in Fig. 5). Note that all excited states under consideration are bound, at least along the chosen coordinate, with minima close to that of the ground state. Interestingly, the depth of the potential well is smaller for the states localized

Table 3 Energies of selected vertical transitions calculated for the corresponding relaxed geometry of IrPS or IrPS–Ag_n (in eV) as well as their oscillator strengths (in parentheses). Note that some transitions have not been found among the lowest excited states considered

Singlet–singlet				
	$d_{x^2-y^2} \rightarrow \pi_1^*$(bpy)	$d_{x^2-y^2} \rightarrow \pi_1^*$(ppy)	$d_{yz} \rightarrow \pi_1^*$(bpy)	π_1(bpy) $\rightarrow \pi_1^*$(bpy)
IrPS[28]	3.46 (0.000)	3.90 (0.123)	4.03 (0.000)	4.84 (0.138)[a]
IIa	3.74 (0.000)	4.07 (0.120)	4.13 (0.001)	—
IVa	3.59 (0.000)	4.01 (0.089)[d]	4.15 (0.001)[g]	—
VIa	3.72 (0.021)	4.08 (0.064)	4.13 (0.000)	—
Singlet–triplet				
	$d_{x^2-y^2} \rightarrow \pi_1^*$(bpy)	$d_{x^2-y^2} \rightarrow \pi_1^*$(ppy)	$d_{yz} \rightarrow \pi_1^*$(bpy)	π_1(bpy) $\rightarrow \pi_1^*$(bpy)
IrPS[28]	3.45	2.95[a,b]	3.97[a]	3.13
IIa	3.73	—	4.03[a]	3.16
IVa	3.64[d]	3.76[a,d]	—	3.15
VIa	3.68	3.02[c,d]	—	3.15
Doublet–doublet				
	$d_{x^2-y^2} \rightarrow \pi_1^*$(ppy)	π_1^*(bpy) $\rightarrow \pi_2^*$(ppy)	π_1^*(bpy) $\rightarrow \pi_1^*$(ppy)	π_1(bpy) $\rightarrow \pi_1^*$(bpy)
IrPS	2.94 (0.000)	2.47 (0.005)	2.39 (0.000)	—
I	—	1.82 (0.006)	2.00 (0.001)	3.62 (0.000)[d,e]
III	3.77 (0.200)	—	2.53 (0.002)	—
Va	—	—	—	3.98 (0.114)[d,f]

[a] Very complex state of a mixed MLCT and LC (ppy) character can be attributed to both. [b] Also 3.70. [c] Also 3.12. [d] Mixed with IM transitions. [e] Also 3.97 (0.059). [f] Also 4.15 (0.000). [g] Also 2.69 (0.000).

Table 4 Energies of selected vertical transitions calculated for the corresponding relaxed geometry of Ag_n or IrPS-Ag_n (in eV) localized on Ag clusters as well as their oscillator strengths (in parentheses)

	Pure Ag_n	IrPS$\cdots Ag_n$
IIa	3.06 (0.408)	3.36 (0.446)
	4.35 (0.230)	3.94 (0.086)
III	4.17 (0.308)	4.08 (0.387)[a]
IVa	4.15 (0.493)	2.81 (0.533)
	4.57 (0.303)	3.90 (0.247)
Va	3.64 (0.842)	3.19 (0.393)
	3.96 (0.477)	3.92 (0.151)[a]
		3.98 (0.114)[a]
		4.06 (0.167)[a]
VIa	3.13 (0.161)	3.46 (0.734)
	3.71 (1.112)	

[a] Mixed with IM transitions.

either on IrPS or Ag_n, whereas the potentials of the CT states are notably more distance-dependent. The curves have multiple crossings, especially for the Ag → IrPS CT states which implies a complex photodynamics. In general, there is no strong dependence of the oscillator strengths on the R(Ir–Ag) distance. An exception is the σ(Ag) → σ^*(Ag) transitions in IVa and II, where the oscillator strength increases and decreases as a function of R(Ir–Ag), respectively (not shown).

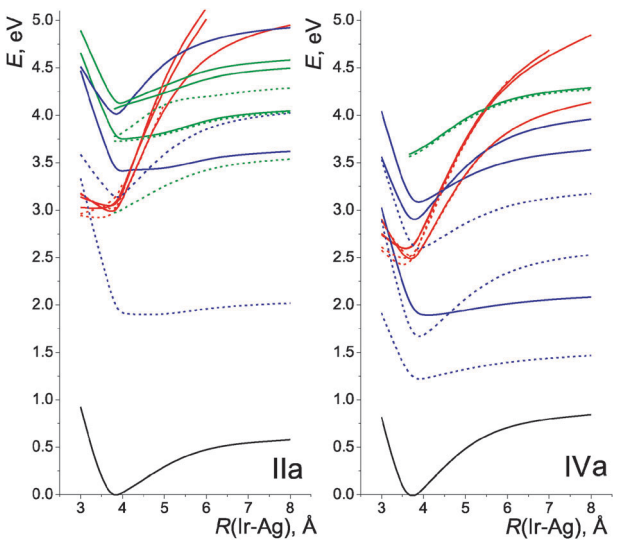

Fig. 5 Potential energy curves (TDDFT/LC-BLYP) of systems IIa and IVa in dependence on the distance between Ir and the closest Ag atom. Solid lines correspond to singlet electronic states; dashed lines correspond to triplet states. Black color: ground state; green: states for which excitation is localized on IrPS; blue: states localized on Ag_n; red: CT between IrPS and Ag_n states.

Discussion

One of the most interesting points to discuss is the application of such combined IrPS–Ag_n systems for photocatalysis. Hence the question to be addressed concerns the extent of modification of the photochemical and photophysical properties of the photosensitizer and how this might influence hydrogen production within a catalytic cycle. The present study has been focused on the initial step of photoabsorption and on the nature of the electronically excited states only. In general, one might argue that the goal should be the enhancement of the absorption cross-section of IrPS with the range of the sun's spectrum. Further, the change in the nature of the excited states, *i.e.* the appearance of long-range CT states might have an impact on the type of electron transfer, which can be realized if the present complex is integrated into a heterogeneous catalytic system.

To summarize the present findings on small silver clusters we have found some changes in the low-energy electronic spectra of constituents and also that new long-range

$Ag_n \leftrightarrow$ IrPS CT states appear. These CT states are numerous and may occur to the red of the locally excited states of IrPS and Ag_n. The long-range CT character of these states may increase the lifetime of corresponding electronic states and may lead to changes in the contributions of radiative and non-radiative deactivation channels for the photocatalyst. Further, we have shown that binding of IrPS to silver clusters takes place not only in the ground state but the lowest excited state potential curves are also of bound character.

For the small metal clusters, no pronounced plasmonic resonance is observed and thus no plasmonic enhancement is expected. Note that in general, the enhancement of absorption is mainly due to the increasing absorption of silver clusters themselves. Similar behaviour was also observed for strongly bound peptide–cluster systems.[3,55,56] If the integrated areas under the calculated absorption spectra of bound complexes are compared with those of the bare IrPS, we can state that in all cases there is an enhancement of absorption from about 20% to 500%. The enhancement increases with the number of silver atoms in the system. But if we subtract the absorption of bare silver clusters, *i.e.* $\sigma_{abs}(IrPS–Ag_n) - \sigma_{abs}(IrPS) - \sigma_{abs}(Ag_n)$, we obtain instead of a strong enhancement a decrease in the integrated absorption by up to 100% or only a slight enhancement (20–120%).

If extrapolated to larger n, *i.e.* clusters with diameter of 10 nm and more, the structure of the low-energy spectrum could have a strong impact on the photophysics and photochemistry of IrPS. The photoinduced dynamics will be determined by the competition between four processes, namely charge-transfer, intersystem crossing (between singlet and triplet states), internal conversion, and energy dissipation in the metal cluster. Spin–orbit effects were not included in the present study, but still we can discuss the principal photophysics. However, these effects should be taken into account when calculating rates of the corresponding processes. Discussing intersystem crossing we rely on the experimental findings that showed this process to be rather effective for Ir organometallic compounds.[57,58] Two interesting scenarios can be discussed as sketched in Fig. 6:

(i) The CT process between IrPS and the (quasi)continuum states of Ag_n is dominant (Fig. 6a). First, IrPS is photoexcited into the singlet manifold (S_n); then follows the cascade of internal conversions to lower singlet states. If one of these states is of IM CT character it leads to the separation of the charges giving both IrPS and Ag_n in, *e.g.*, ground (D_0) and excited (D_l) doublet states. Since the life time of the plasmonic states has been estimated to be about 10 fs,[59] the silver particle would rapidly relax into the lowest doublet state. The excess energy is dissipating in the cluster. However, IrPS stays photoreduced and can be involved in the further catalytic processes. In principle, we observe such a CT for the present small clusters provided that the number of silver atoms is even. For the odd number clusters, such reduced state is achieved already in the ground electronic state. Discussing clusters with a given (odd or even) n we suppose that at least for small n they can be obtained experimentally; for details of mass selection (see *e.g.* ref. 60 and 61).

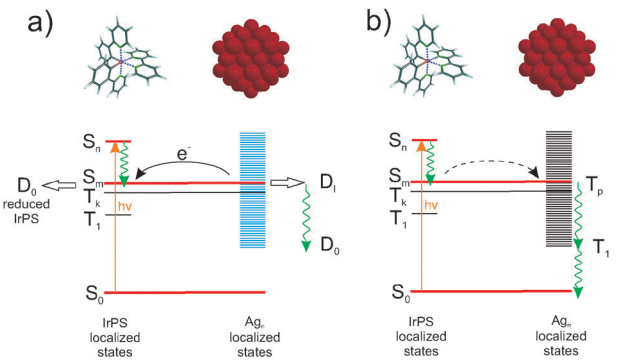

Fig. 6 Two of the possible photophysical processes of the IrPS···Ag_n system with large n: (a) the reduction of IrPS through electron transfer from the Ag_n cluster and (b) dissipation of the excitation energy on the clusters triplet manifold. Black solid arrow: charge transfer; green wavy arrows: internal conversion; black dashed arrow: intersystem crossing. Red bars: singlet states; black bars: triplet states; blue bars: doublet states.

(ii) The rates of the intersystem crossing and further internal conversion to the lowest triplet state (T_1) exceed that of the CT process. In this case the lowest triplet state determines the photophysical behaviour (Fig. 6b). As was shown in this paper, in most cases the lowest triplet state is cluster localized and, thus, one could expect the fast dissipation of excitation energy on the cluster (Fig. 6b). In other words, one would observe a fast loss of photophysical and photochemical activity.

In principle scenario (i) could favour the catalysis of water reduction by means of a new mechanism, where the metal cluster itself act as a sacrificial reductant. In that case, another sacrificial reagent should be added to the photocatalytical system in order to reduce the metal cluster after it has given an electron to IrPS. For compounds containing heavy elements, like Ir or analogous metals, due to effective intersystem crossing one should probably expect the scenario (ii). However, for organic dyes containing light elements the dynamics can occur on the singlet manifold and long-range CT could play an important role leading to scenario (i).

Conclusions

The study of the interaction of IrPS and small silver clusters, Ag_n (n = 1–6), yielded a scenario of weak physisorption with the preferable location of Ag_n in cavities between the ligands. Electronic properties are found to oscillate with the number of silver atoms. An interesting aspect of the considered systems with an odd number of silver atoms is the "redox" nature of their ground electronic states: $IrPS^0 \cdots Ag_n^+$. This situation corresponds to different HOMO and LUMO orbitals for systems with odd and even number of silver atoms, which implies different directions of CT in the lowest electronic transitions. The structure of absorption spectra of IrPS···Ag_n systems notably differs from those of the isolated parts. This difference is not connected with strong changes in the transitions localized on either photosensitizer or silver cluster, but related to the appearance of the intermolecular long-range CT electronic states between IrPS and Ag_n. These states might have an influence on subsequent photochemical and photophysical processes involving the lowest excited states. The energetic position of these states is only slightly dependent on the relative orientation of IrPS and Ag_n, but strongly varies with the distance between them. The calculated potential energy curves for the excited states imply rather complex photodynamics.

Furthermore, depending on the relative rates of charge transfer, intersystem crossing, internal conversion, and energy dissipation on the cluster particle new photocatalytic schemes might be possible, but also a strong quenching of photoprocesses.

Acknowledgements

This work has been financially supported by the ESF project "Nanostructured Materials for Hydrogen Production (Nano4-Hydrogen)" and the BMBF ("Spitzenforschung und Innovation in den Neuen Ländern"), project "Light2Hydrogen".

References

1 E. Katz and I. Willner, *Angew. Chem., Int. Ed.*, 2004, **43**, 6042–6108.
2 N. T. Fofang, T.-H. Park, O. Neumann, N. A. Mirin, P. Nordlander and N. J. Halas, *Nano Lett.*, 2008, **8**, 3481–3487.
3 A. Kulesza, R. Mitrić and V. Bonačić-Koutecký, *J. Phys. Chem. A*, 2009, **113**, 3783–3788.
4 S. I. Shopova, R. Rajmangal, S. Holler and S. Arnold, *Appl. Phys. Lett.*, 2011, **98**, 243104.
5 Z. Liu, W. Hou, P. Pavaskar, M. Aykol and S. B. Cronin, *Nano Lett.*, 2011, **11**, 1111–1116.
6 P. Anger, P. Bharadwaj and L. Novotny, *Phys. Rev. Lett.*, 2006, **96**, 113002.
7 S. Bhowmick, S. Saini, V. B. Shenoy and B. Bagchi, *J. Chem. Phys.*, 2006, **125**, 181102.
8 W. Gu, H. Choi and K. K. Kim, *J. Phys. Chem.*, 2007, **111**, 8121–8125.
9 A. M. Kelley, *J. Chem. Phys.*, 2008, **128**, 224702.
10 L. Jensen, L. L. Zhao and G. C. Schatz, *J. Phys. Chem. C*, 2007, **111**, 4756–4764.
11 A. Trügler and U. Hohenester, *Phys. Rev. B: Condens. Matter Mater. Phys.*, 2008, **77**, 115403.
12 J. Yu, S. A. Patel and R. M. Dickson, *Angew. Chem., Int. Ed.*, 2007, **46**, 2028–2030.
13 S.-I. Tanaka, J. Miyazaki, D. K. Tiwari, T. Jin and Y. Inouye, *Angew. Chem., Int. Ed.*, 2011, **50**, 431–435.
14 C. M. Aikens, S. Li and G. C. Schatz, *J. Phys. Chem. C*, 2008, **112**, 11272–11279.
15 D. Mollenhauer, J. Flob, H.-U. Reissig, E. Voloshina and B. Paulus, *J. Comput. Chem.*, 2011, **32**, 1839–1845.
16 L. S. Hung and C. H. Chen, *Mater. Sci. Eng., R*, 2002, **39**, 143–222.
17 L. L. Tinker, N. D. McDaniel, P. N. Curtin, C. K. Smith, M. J. Ireland and S. Bernhard, *Chem.–Eur. J.*, 2007, **13**, 8726–8732.
18 P. N. Curtin, L. L. Tinker, C. M. Burgess, E. D. Cline and S. Bernhard, *Inorg. Chem.*, 2009, **48**, 10498–10506.
19 M. S. Lowry, J. I. Goldsmith, J. D. Slinker, R. Rohl, R. A. Pascal Jr, G. G. Malliaras and S. Bernhard, *Chem. Mater.*, 2005, **17**, 5712–5719.
20 J. I. Goldsmith, W. R. Hudson, M. S. Lowry, T. H. Anderson and S. Bernhard, *J. Am. Chem. Soc.*, 2005, **127**, 7502–7510.
21 F. Gärtner, B. Sundararaju, A.-E. Surkus, A. Boddien, B. Loges, H. Junge, P. H. Dixneuf and M. Beller, *Angew. Chem., Int. Ed.*, 2009, **48**, 9962–9965.
22 S. Tschierlei, M. Karnahl, M. Presselt, B. Dietzek, J. Guthmuller, L. González, M. Schmitt, S. Rau and J. Popp, *Angew. Chem., Int. Ed.*, 2010, **49**, 3981–3984.
23 K.-C. Tang, K. L. Liu and I.-C. Chen, *Chem. Phys. Lett.*, 2004, **386**, 437–441.
24 G. J. Hedley, A. Ruseckas and D. W. Samuel, *J. Phys. Chem. A*, 2009, **113**, 2–4.
25 M. G. Colombo, A. Hauser and H. U. Güdel, in *Electronic and Vibronic Spectra of Transition Metal Complexes I*, Springer, Berlin/Heidelberg, 1994, vol. 171, pp. 143–171.
26 A. P. Wilde, K. A. King and R. J. Watts, *J. Phys. Chem.*, 1991, **95**, 629–634.
27 S.-H. Wu, J.-W. Ling, S.-H. Lai, M.-J. Huang, C. H. Cheng and I.-C. Chen, *J. Phys. Chem. A*, 2010, **114**, 10339–10344.
28 S. I. Bokarev, O. S. Bokareva and O. Kühn, 2011, submitted for publication.
29 P. J. Hay and W. R. Wadt, *J. Chem. Phys.*, 1985, **82**, 270–283.
30 W. J. Hehre, R. Ditchfield and J. A. Pople, *J. Chem. Phys.*, 1972, **56**, 2257–2261.
31 P. C. Hariharan and J. A. Pople, *Theor. Chim. Acta*, 1973, **28**, 213–222.
32 A. Dreuw and M. Head-Gordon, *Chem. Rev.*, 2005, **105**, 4009–4037.
33 M. J. G. Peach, P. Benfield, T. Helgaker and D. J. Tozer, *J. Chem. Phys.*, 2008, **128**, 044118.
34 H. Iikura, T. Tsuneda, T. Yanai and K. Hirao, *J. Chem. Phys.*, 2001, **115**, 3540–3544.
35 Y. Tawada, T. Tsuneda, S. Yanagisawa, T. Yanai and K. Hirao, *J. Chem. Phys.*, 2004, **120**, 8425–8433.
36 M. Chiba, T. Tsuneda and K. Hirao, *J. Chem. Phys.*, 2006, **124**, 144106.
37 J. P. Perdew, K. Burke and M. Ernzerhof, *Phys. Rev. Lett.*, 1996, **77**, 3965–3968.
38 J. P. Perdew, K. Burke and M. Ernzerhof, *Phys. Rev. Lett.*, 1997, **78**, 1396.
39 C. Adamo and V. Barone, *J. Chem. Phys.*, 1999, **110**, 6158–6170.
40 A. D. Becke, *J. Chem. Phys.*, 1993, **98**, 1372–1377.
41 T. Yanai, D. P. Tew and N. C. Handy, *Chem. Phys. Lett.*, 2004, **393**, 51–57.
42 Y. Zhao and D. G. Truhlar, *J. Phys. Chem. A*, 2006, **110**, 13126–13130.
43 S. E. Wheeler and K. N. Houk, *J. Chem. Theory Comput.*, 2010, **6**, 395–404.
44 S. F. Boys and F. Bernardi, *Mol. Phys.*, 1970, **19**, 553–566.
45 S. Simon, M. Duran and J. J. Dannenberg, *J. Chem. Phys.*, 1996, **105**, 472902.
46 M. W. Schmidt, K. K. Baldridge, J. A. Boatz, S. T. Elbert, M. S. Gordon, J. H. Jensen, S. Koseki, N. Matsunaga, K. A. Nguyen, S. Su, T. L. Windus, M. Dupuis and J. A. Montgomery Jr., *J. Comput. Chem.*, 1993, **14**, 1347–1363.
47 V. Bonačić-Koutecký, L. Češpiva, P. Fantucci and J. Koutecký, *J. Chem. Phys.*, 1993, **98**, 7981–7994.
48 V. Bonačić-Koutecký, V. Veyret and R. Mitrić, *J. Chem. Phys.*, 2001, **115**, 10450–10460.
49 R. Mitrić, M. Hartmann, B. Stanca, V. Bonačić-Koutecký and P. Fantucci, *J. Phys. Chem. A*, 2001, **105**, 8892–8905.
50 R. Fournier, *J. Chem. Phys.*, 2001, **115**, 2165–2177.
51 M. Harb, F. Rabilloud, D. Simon, A. Rydlo, S. Lecoultre, F. Conus, V. Rodrigues and C. Félix, *J. Chem. Phys.*, 2008, **129**, 194108.
52 J. C. Idrobo, S. Öğüt and J. Jellinek, *Phys. Rev. B: Condens. Matter Mater. Phys.*, 2005, **72**, 085445.
53 K. A. King and R. J. Watts, *J. Am. Chem. Soc.*, 1987, **109**, 1589–1590.
54 E. M. Fernández, J. M. Soler, I. L. Garzón and L. C. Balbás, *Phys. Rev. B: Condens. Matter Mater. Phys.*, 2004, **70**, 165403.
55 T. Tabarin, A. Kulesza, R. Antoine, R. Mitrić, M. Broyer, P. Dugourd and V. Bonačić-Koutecký, *Phys. Rev. Lett.*, 2008, **101**, 213001.
56 R. Mitrić, J. Petersen, A. Kulesza, V. Bonačić-Koutecký, T. Tabarin, I. Compagnon, R. Antoine, M. Broyer and P. Dugourd, *Chem. Phys.*, 2008, **343**, 372–380.
57 G. J. Hedley, A. Ruseckas and I. D. W. Samuel, *Chem. Phys. Lett.*, 2008, **450**, 292–296.
58 W. J. Finkenzeller, P. Stößel and H. Yersin, *Chem. Phys. Lett.*, 2004, **397**, 289–295.
59 B. Lambrecht, A. Leitner and F. R. Aussenegg, *Appl. Phys. B: Lasers Opt.*, 1997, **64**, 269–272.
60 M. Couillard, S. Pratontep and R. E. Palme, *Appl. Phys. Lett.*, 2003, **82**, 2595.
61 L. Benz, X. Tong, P. Kemper, Y. Lilach, A. Kolmakov, H. Metiu, M. T. Bowers and S. K. Buratto, *J. Chem. Phys.*, 2005, **122**, 081102.

